Chemical Science

Dynamic Article Links ►

Cite this: DOI: 10.1039/c0xx00000x

www.rsc.org/xxxxxx

EDGE ARTICLE

EuroTracker Dyes: Highly Emissive Europium Complexes as Alternative Organelle Stains for Live Cell Imaging†

Stephen J. Butler[a], Laurent Lamarque[b], Robert Pal[a] and David Parker*[a]

Received (in XXX, XXX) Xth XXXXXXXXX 2013, Accepted Xth XXXXXXXXX 2013

DOI: 10.1039/b000000x

Nine very bright europium(III) complexes with different macrocyclic ligands have been prepared that exhibit excellent cell uptake behaviour and distinctive sub-cellular localisation profiles, allowing the use of fluorescence microscopy and time-gated spectral imaging to track their fate *in cellulo*. Their use as cellular imaging stains is described for the selective illumination of mitochondria, lysosomes or the endoplasmic reticulum of various mammalian cell types.

Introduction

We report very bright Eu complexes that are attractive alternatives to commercial fluorescent dyes for live cell imaging.

In order to investigate intracellular and sub-cellular processes, fluorescent stains are needed that can visualise particular cellular compartments with high spatial and temporal resolution. A major challenge in live cell imaging is the creation of selective stains – compounds that enter cells and localise preferentially to a particular organelle without perturbing cell homeostasis. This is a critical requirement not only for cell imaging but for any species being considered as a diagnostic or therapeutic agent. One approach to this problem involves the conjugation of a targeting moiety to the emissive compound, such as an arginine-rich cell-penetrating peptide or a nuclear localisation sequence (NLS) peptide.[1-5] The targeting vector is reputed to facilitate cell uptake and in certain cases promotes trafficking to a specific organelle, through non-covalent interactions with a carrier protein. The second strategy does not involve a targeting functionality but relies upon systematic variation of the chemical structure of a parent compound and screening of the intrinsic probe distribution in different cell types.[6,7] This approach has been developed for a number of fluorescent organic dyes commonly used in cell biology to visualise selected organelles, notably the MitoTracker™ and LysoTracker™ family of stains that reveal the mitochondria and lysosomes selectively.

The MitoTracker stains are based upon substituted benzylic chlorides that irreversibly alkylate Cys residues in abundant mitochondrial proteins (e.g. heat shock protein-60, VDAC-1, aldolase-A)[8a] and probably also attack mitochondrial DNA, *via* alkylation at guanine N-7. These reactions inevitably result in perturbation of normal organelle function. Indeed, live cell staining experiments using these dyes need to be performed within 30 minutes, after which cell homeostasis may be irreversibly changed. Another drawback of commercial dyes and fluorescent proteins is photobleaching, in which the dye intensity decreases rapidly as a function of the exposure time to the excitation light, inhibiting their use in time-lapsed live cell or fixed specimen imaging experiments. To circumvent these issues, alternative luminescent stains are needed that are non-invasive and less prone to photobleaching.

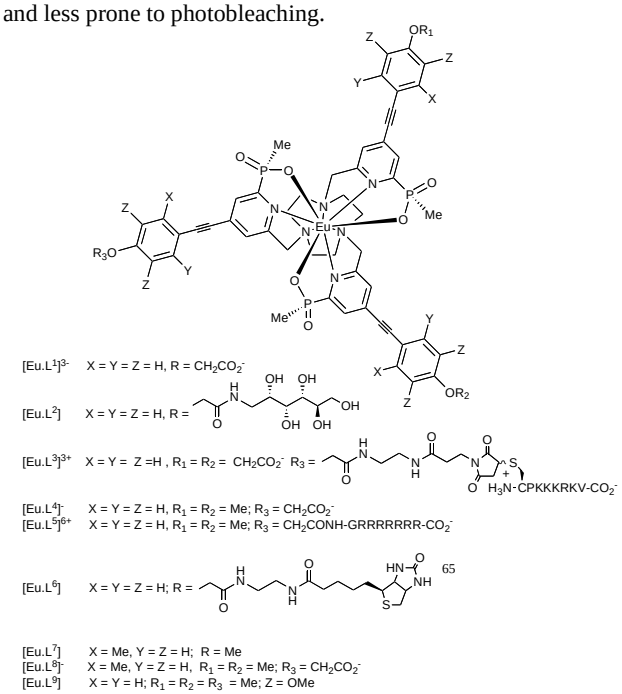

Fig. 1. Structures of europium(III)-based cellular stains [**Eu.**L[1-9]]

Over the last decade, emissive metal coordination complexes have emerged as a distinctive class of intracellular stains and probes.[8-26] Complexes of the lanthanide(III) ions offer particular scope in this respect,[17-26] as they possess several advantages over conventional fluorescent dyes, including a large Stokes' shift that

minimizes self-quenching and an optical signal that conveys information about the local environment through changes in emission spectral form and lifetime. A key feature of luminescent lanthanide(III) complexes is the longer lifetime of emission; this permits the use of time-gated detection methods to eliminate short-lived autofluorescence from biomolecules, generating high quality images. Recently, we introduced a new class of highly emissive europium complexes, with extinction coefficients in the range 55-60,000 $M^{-1}cm^{-1}$ (330 to 350 nm) and an emission quantum yield in methanol of around 50%.[27] Due to their high brightness, these systems show promise as intracellular stains, allowing rapid spectral imaging acquisition using CCD detectors.

In this work, we report a series of structurally related Eu complex-conjugates (Figure 1) and demonstrate their utility as selective organelle stains, e.g. for the mitochondria, lysosomes and endoplasmic reticulum. Each Eu complex is based on a triazacyclononane core with three pyridyl methylphosphinate groups functionalised with strongly absorbing arylalkynyl sensitisers. At least one aryl alkynyl sensitiser is functionalised at the *para*-position with a carboxylic acid group, allowing conjugation with different hydrophilic moieties or targeting vectors. Complex [**Eu.L^{6}**] was labelled with a biotin derivative to enable selective FRET experiments to be undertaken *in cellulo*, *via* non-covalent binding between the biotinylated complex (donor) and a commercial streptavidin-fluorophore conjugate (acceptor).

Synthesis

The C_3-symmetrical europium complexes [**Eu.L^{1}**]$^{3-}$, [**Eu.L^{2}**], [**Eu.L^{7}**] and [**Eu.L^{9}**] were synthesized using established methodology.[27, 28]The Eu-NLS peptide conjugate [**Eu.L^{3}**]$^{3+}$ was prepared from the anionic complex [**Eu.L^{1}**]$^{3-}$ in two steps with a view to staining the nucleus, as the NLS sequence reputedly directs transport. First, [**Eu.L^{1}**]$^{3-}$ was activated using 1 equivalent of PyBOP and coupled with the 2-aminoethyl derivative of N-carboxypropylmaleimide in anhydrous DMF to afford the corresponding maleimide conjugate. Subsequent reaction with the N-terminal thiol group of the NLS peptide, Cys-Gly-Pro-$(Lys)_3$-Arg-Lys-Val, in a mixture of DMSO/aqueous phosphate buffer (50 mM, pH 7, 6 h), afforded [**Eu.L^{3}**]$^{3+}$ in good yield after purification by preparative RP-HPLC. The unsymmetrical complexes [**Eu.L^{4}**]$^{-}$ and [**Eu.L^{8}**]$^{-}$ were prepared in a stepwise manner in which the sensitising group bearing a terminal carboxylic acid was introduced last, following deprotection of mono-BOC-triazacyclononane. Subsequent coupling of [**Eu.L^{4}**]$^{-}$ with the N-terminus of the hydrophilic peptide $Gly\text{-}Arg_7$ or a biotin derivative using PyBOP as the coupling reagent gave the desired conjugates, [**Eu.L^{5}**]$^{6+}$ and [**Eu.L^{6}**] in good yields after purification by reverse-phase HPLC. Each complex exhibits highly efficient emission (Φ_{Total} = 44–55% in MeOH;17 to 26% in water) and a large extinction coefficient (ε_{max} 55-62,000 $M^{-1}cm^{-1}$) (Table 1). Introduction of an *ortho*-methyl substituent in complexes [**Eu.L$^{7\text{-}8}$**] shifts the broad absorption maximum to 340 nm, which is more suited to excitation at 355 or 365 nm (Figure 2). The lifetime of the europium emission was 1.05 (±0.04) ms in water for each complex, consistent with effective shielding of the excited europium ion from intermolecular quenching.

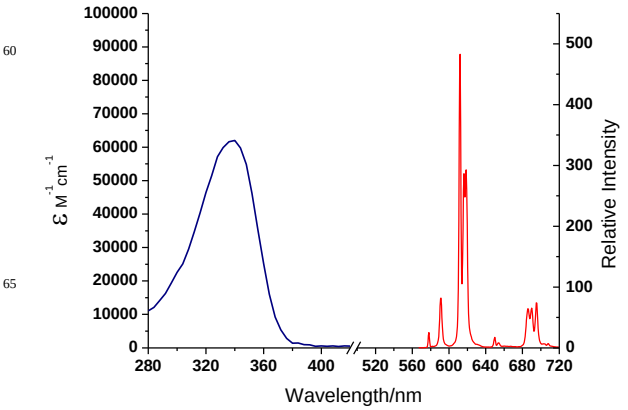

Fig. 2. Absorption and total emission spectrum of [**Eu.L^{7}**] in MeOH (295K)

Table 1. Selected photophysical data for Eu complexes [**Eu.L$^{1\text{-}9}$**] (295K, MeOH). Values in parentheses refer to measurements in water at pH 6.5.

Complex	λ_{max}/ nm	ε/mM^{-1} cm^{-1}	ϕ_{em}/% [a]	τ/ms [a]
[**Eu.L^{1}**]$^{3-}$	330	56.6	44 (26)	1.10 (1.05)
[**Eu.L^{2}**]	328	56.5	50 (26)	1.22 (1.07)
[**Eu.L^{3}**]$^{2+}$	328	58.2	44 (17)	1.14 (1.03)
[**Eu.L^{4}**]$^{-}$	330	60.4	49 (26)	1.22 (1.04)
[**Eu.L^{5}**]$^{5+}$	330	56.4	50 (26)	1.12 (1.04)
[**Eu.L^{6}**]	330	59.0	48 (25)	1.23 (1.07)
[**Eu.L^{7}**]	340	62.0	54 (22)	1.14 (1.01)
[**Eu.L^{8}**]$^{-}$	342	61.9	55 (17)	1.15 (1.00)
[**Eu.L^{9}**]	332	56.4	47 (22)	1.15 (0.91)

[a] errors on quantum yields and lifetimes are ±15%.

Cell Uptake and Localisation Studies

A detailed investigation of the cellular behaviour of each complex was conducted in several different cell types, including mouse skin fibroblasts (NIH-3T3), Chinese hamster ovarian cells (CHO), human prostate adenocarcinoma (PC3) and human breast carcinoma (MDA-MB-231) cells using fluorescence and laser scanning confocal microscopy.

Mitochondrial Staining

Incubation of the neutral complex [**Eu.L^{2}**] (18 μM) in both CHO and NIH-3T3 cells resulted in rapid uptake of the complex and localisation in the mitochondria, verified by co-localisation studies with MitoTracker Green™ (Figure 3). Using phase-modulated resolution enhancement, it was possible to clearly visualise the complex network of mitochondrial tubules, with 80 nm resolution (ESI). Imaging of the mitochondria was possible over extended time periods, and live cells were observed over a period of 48 h, using periodic excitation at low power (e.g. 4 to 8 mW), during which time cell proliferation was not inhibited (IC_{50} > 100 μM (24h)). Selective staining of [**Eu.L^{2}**] to the mitochondria is primarily associated with the amphipathic nature of the complex, and the excellent tolerance may be attributed, in part, to the presence of the peripheral glucamide substituents. The selective mitochondrial localisation could be tentatively attributed to local phosphorylation of the sugar primary OH groups, leading

to an anionic complex that only slowly escapes the mitochondrial organelle.[11b]

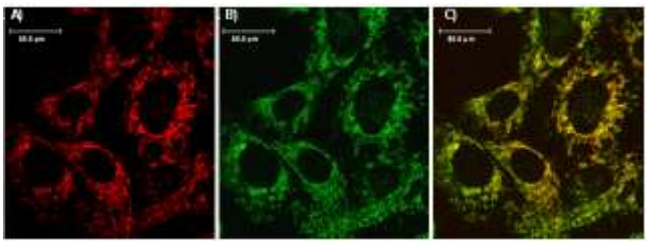

Fig.3 LSCM images showing: (a) mitochondrial localisation of [**Eu.L^2**] of NIH-3T3 cells (1h, 18 μM, λ_{exc} 355 nm, λ_{em} 605–720 nm); (b) MitoTracker Green (λ_{exc} 488 nm, λ_{em} 500–530 nm); (c) RGB merged image showing co-localisation (P = 0.95).

A similar localisation profile was observed for [**Eu.L^7**]. In this case, uptake was slower than for [**Eu.L^2**], with an approx. 40% increase in emission intensity observed between a 4 h and 24 h incubation period.

Analysis of ICP-MS data showed that for 4x10^6 NIH-3T3 cells incubated with [**Eu.L^2**] (18 μM), each cell contained 34 μM of Eu at 24 h, substantially higher than that of [**Eu.L^7**] (6 μM) under the same conditions. Despite the lower uptake of [**Eu.L^7**], equally bright images were obtained after 24 h, due to the higher λ_{max} of this complex (340 nm versus 330 nm for [**Eu.L^2**]), which lies closer to the excitation wavelength of the 355 nm laser used in laser scanning microscopy. Using a 3-dimensional reconstruction plug-in for use with ImageJ software, high resolution (80 nm resolution) 3-D images of [**Eu.L^7**] were created from the recorded *z*-stack images (see ESI).

The mono-anionic complexes [**Eu.L^4**]$^-$ and [**Eu.L^8**]$^-$ and the neutral complex [**Eu.L^9**] also showed mitochondrial localisation at early time points (30 min – 4h loading); however, after a 12 h incubation period, each complex showed a predominant distribution in the endoplasmic reticulum, as confirmed by co-localisation experiments with ER-Tracker Green. Comparison of the ICP-MS data revealed that almost twice the amount of [**Eu.L^8**]$^-$ (17 μM) was internalised by NIH-3T3 cells relative to [**Eu.L^4**]$^-$ (9 μM) under the same experimental conditions.

Lysosomal Staining

The anionic complex [**Eu.L^1**]$^{3-}$ (30 μM) was rapidly internalised by different cell types (NIH-3T3, CHO) and microscopy images taken after a 30 minute incubation revealed preferential accumulation within the lysosomes. Co-localisation studies with LysoTracker-Green indicated clear staining of the lysosomes (Figure 4). A more intense staining was observed after a 12 h incubation, with [**Eu.L^1**]$^{3-}$ retaining its selectivity for the lysosomes. In this case, the negatively charged ancillary ligands serve to both enhance water solubility and help maintain the localization of the complex in the lysosomes. With the biotin conjugate, [**Eu.L^6**], a predominant lysosomal staining was apparent, but with actin-like staining also evident. In the case of complex [**Eu.L^3**]$^{3+}$, the attachment of the NLS peptide did not promote nuclear import. Instead, a predominant lysosomal staining was observed. Unlike every other complex tested, the NLS-conjugate [**Eu.L^3**]$^{3+}$ effectively compromised cell function; cells were held in an arrested telophase state after 12 h and analysis of its cytotoxicity revealed an IC_{50} = 1(±0.1) μM. This represents a dramatic increase in cell toxicity compared to all other Eu complexes studied, which had IC_{50} values of greater than 100 μM and remained localized in live cells over prolonged time periods (up to 48 h) (Table 2).

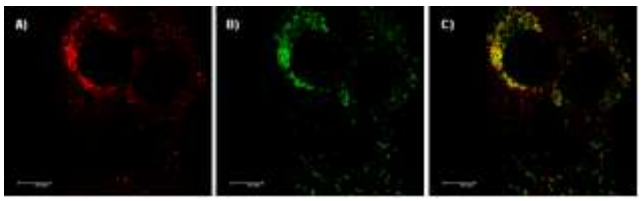

Fig.4 LSCM images showing: (a) lysosomal localisation of [**Eu.L^1**]$^{3-}$ in NIH-3T3 cells (8h, 30 μM, λ_{exc} 355 nm, λ_{em} 605–720 nm); (b) LysoTracker Green (λ_{exc} 514 nm, 530–550 nm); (c) RGB merge image showing co-localisation (P = 0.81).

Endoplasmic Reticulum Staining

Following 1 h incubation, the polyarginine complex [**Eu.L^5**]$^{6+}$ (10 μM) exhibited efficient localisation to the mitochondria of NIH-3T3 and CHO cells, with subsequent trafficking to the endoplasmic reticulum over extended time periods (12-24 h). However, accelerated staining of the endoplasmic reticulum was achieved by the addition of the known stimulator of macropinocytosis, 1,2-diapalmitoyl-*rac*-diacylglycerol (500 ng/mL), to the growth media. Under these conditions, a clear ER localisation was evident (30 min incubation), confirmed by co-localisation of [**Eu.L^5**]$^{6+}$ with ER-Tracker green (Figure 5).

Microscopy images of [**Eu.L^5**]$^{6+}$ taken after a 1 h incubation period suggested a modest increase in emission intensity relative to the parent compound [**Eu.L^4**]$^-$. The ICP-MS analysis, however, revealed that an average NIH-3T3 cell treated with [**Eu.L^5**]$^{6+}$ (10 μM) contained 1.6 μmol of Eu(III), the same as that of the [**Eu.L^4**]$^-$ (1.8 μM) under the same conditions. Thus, the attachment of the polyarginine peptide to [**Eu.L^4**]$^-$ neither significantly affected the inherent uptake nor perturbed the intracellular distribution of this complex.

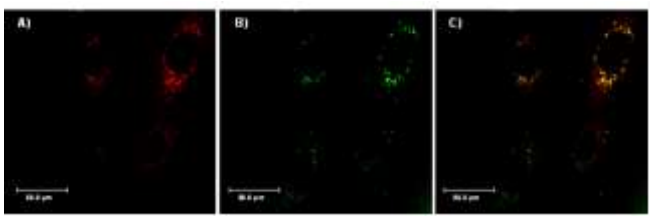

Fig.5 LSCM images showing: (a) staining of the endoplasmic reticulum of NIH-3T3 cells with [**Eu.L^5**]$^{6+}$ (30 min, 10 μM, λ_{exc} 355 nm, λ_{em} 605–720 nm); (b) ER-Tracker Green (λ_{exc} 496 nm, 505–535 nm); (c) RGB merge image showing co-localisation (P = 0.88).

Mechanism of Cell Uptake and Cytotoxicity

To understand the mechanism of cell uptake, the behaviour of selected representative complexes was examined in the presence of known inhibitors and promoters of defined cell-uptake pathways.[7, 29] In each case, the extent of intracellular uptake was evaluated first by comparing the observed image intensity using LSCM microscopy and then by measuring the amount of Eu(III)

in sorted and counted cell populations using ICP-MS (Table 2).

Table 2. ICP-MS data and cytotoxicity data for complexes [**Eu.L$^{1\text{-}8}$**]

Complex	$C_{loading}$/μM[a]	C_{cell}/μM[a]	Accumulation/%	IC_{50}/μM[c]
[**Eu.L^{1}**]$^{3-}$	30	11	36	> 100
[**Eu.L^{2}**]	15	34	165	> 100
[**Eu.L^{3}**]$^{2+}$	10	1.4	14	1
[**Eu.L^{4}**]$^{-}$	30	9.3	31	> 100
[**Eu.L^{5}**]$^{6+}$	15	23	151	> 100
[**Eu.L^{6}**]	10	7.1	71	> 100
[**Eu.L^{7}**]	30	6.3 (4.1)[b]	21	> 100
[**Eu.L^{8}**]$^{-}$	30	17 (6.3)[b]	55	> 100

ICP-MS data were recorded after a 24 h incubation period; [a] errors on ICP-MS measurements are ±10%; [b] measured after a 4 h incubation period; [c] IC_{50} values were assessed using the MTT colorimetric assay. The cells were incubated with each complex in the concentration range 0.01 to 100 μM. Errors in IC_{50} values are ±10%

When the specific pathway of macropinocytosis was inhibited (by incubation with wortmannin[30] or amiloride[31]), a marked decrease (typically 20-30%) in the cellular uptake was observed for complexes [**Eu.L$^{1\text{-}5}$**], in different cell types (CHO, NIH-3T3). This effect was most pronounced for the poly-Arg conjugate [**Eu.L^{5}**]$^{6+}$, for which a 60% decrease in emission intensity was observed. The addition of known stimulators of macropinocytosis to the growth media (phorbol esters and 1,2-dipalmitoyl-*rac*-diacylglycerol)[32] resulted in enhanced uptake (up to 40%) of each complex, except for [**Eu.L^{6}**] which showed no change. Macropinocytosis is a form of endocytosis involving the formation of leaky macropinosomes of irregular size and shape, the contents of which are released into the cytoplasm. This uptake pathway represents an attractive means for the delivery of the luminescent complexes within the cell, as the dyes can readily escape from the macropinosome, permitting vesicular trafficking to other compartments.[33] Uptake of the biotin conjugate [**Eu.L^{6}**] was not inhibited by wortmannin or amiloride. Furthermore, ICP-MS studies revealed that approximately 50% of the accumulated complex egressed into the cell growth medium (significant amounts were also observed by spectral acquisition of the complex in the external medium). Such behaviour is consistent with a dominant, biotin-specific uptake mechanism.

Tracking the biotin-avidin interaction inside cells using FRET

Due to the spectral overlap of the hypersensitive ΔJ = 2 manifold of [**Eu.L^{6}**] (620 ± 10 nm) and the absorption spectrum of Streptavidin AlexaFluor633 (SA-AF633) (λ_{exc} 633 nm, λ_{em} 650 nm), these two components were used as a FRET donor and acceptor respectively,[34] in a model experiment to track the interaction between streptavidin and biotin in cells. Before the key FRET experiments were undertaken, the fluorescence behaviour of SA-AF633 was assessed and any autofluorescence quantified that may arise from endogenous donor molecules excited at 355 nm. First, NIH-3T3 cells were cultured in DMEM cell growth medium containing neither biotin nor phenol red, and incubated with SA-AF633 (380 nM) for 1 h. Microscopy images (λ_{exc} 633 nm, λ_{em} 650–670 nm) revealed predominant staining of the streptavidin tag in the lysosomes, confirmed by co-staining with LysoTracker Green. Next, simultaneous incubation of [**Eu.L^{6}**](15 μM) and SA-AF633 (380 nM) in the same medium for 1h led to rapid internalization of the biotin complex-streptavidin pair, as revealed by the observed FRET induced signal (λ_{exc} 355 nm, λ_{em} 655−680 nm) between the two components (Figure 6). Microscopy images of the FRET pair (λ_{exc} 355 nm, λ_{em} 605–630 nm) showed a 300% increase in emission intensity relative to [**Eu.L^{6}**] alone under the same conditions. This intensity increase was corroborated by ICP-MS analysis, which showed a two-fold increase in uptake of the complex when the donor/acceptor pair were loaded simultaneously, indicating that the SA-AF633 promotes the active internalisation of [**EuL^{6}**]. Localisation of the dye pair within the lysosomes was observed, with actin-like staining also evident. Finally, consecutive incubation with [**Eu.L^{6}**] (1h, 15 μM) and SA-AF633 (380 nM, 30 min), interspersed by a rapid wash with fresh medium (<2 min), gave rise to a 200% increase in observed Eu emission intensity. Under these conditions, a 1.3 fold increase in uptake of [**Eu.L^{6}**] was measured by ICP-MS analysis. This behaviour is unsurprising, given that [**Eu.L^{6}**] was shown to egress into the growth medium; thus, any Eu complex present in the medium may be transported back into the cell with the assistance of the Streptavidin Alexafluor. Very similar lysosomal co-localisation behaviour was observed, as in Figure 6 (see ESI).

The same behaviour was exhibited when the order of addition of donor and acceptor was reversed; a 180% increase in Eu emission intensity was observed, with clear evidence for lysosomal FRET. The acceptor emitted with a much longer lifetime following energy transfer from the Eu complex (λ_{exc} 355 nm).

Fig.6 LSCM images (scale bar 17 μm)showing: (a) localisation of [**Eu.L^{6}**] in

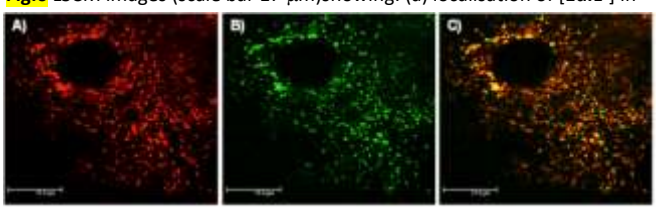

the lysosomes of NIH-3T3 cells (1h, 15 μM, λ_{exc} 355 nm, λ_{em} 600–630 nm); (b) FRET induced SA-AF633 fluorescence (λ_{exc} 355 nm, λ_{em} 655−680 nm); (c) RGB merge image showing co-localisation of the donor-acceptor pair (P = 0.93).

Upon quenching of the Eu emission by energy transfer to the AlexaFluor-633 dye, SA-AF633, a decrease in the lifetime of the donor [**Eu.L^{6}**] is expected, accompanied by a dramatic increase in the emission lifetime of the acceptor, from its intrinsic value of ca. 40 ns. To confirm this, the change in lifetime of the biotin complex [**Eu.L^{6}**] in cells was measured, when incubated in the absence and presence of SA-AF633. The lifetime of [**Eu.L^{6}**] in cells when incubated alone was measured to be 880 μs which decreased to 525 μs due to FRET quenching. The Eu lifetime modulation was observed at 610-630 nm using a modified Zeiss Axiovert 200M microscope, equipped with a 365 nm pulsed UV-LED excitation source and a cooled PMT detector. By changing the detection window to 660-680 nm, the SA-AF633 lifetime was found to be 75 μs (Figure 7).

These experiments constitute a rare example of a time-resolved intracellular FRET experiment, using a lanthanide complexes as the donor [35], and serve to highlight the potential for

future experiments of this type, wherein the lanthanide complex is targeted to a particular organelle to report a biochemical event.

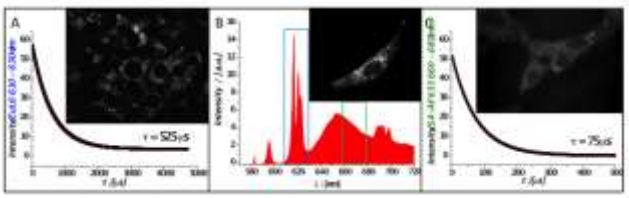

Fig.7 (a) Lifetime of [**Eu.L^6**] (15 μM) as a FRET donor (λ_{exc} 365 nm, observed at 610-630 nm); (b) time-gated (t_g = 5 μs) spectrum of [**Eu.L^6**] (15 μM) and SA-AF633 (380 nM); (c) lifetime of SA-AF633 (380 nM) following FRET from the Eu donor (λ_{exc} 365 nm, observed at 660-680 nm). Each of the above were recorded in NIH-3T3 cells (16 cells in the field of view) at 1 h after simultaneous loading of the donor and acceptor. Inserts show time-gated (t_g = 5 μs) fluorescence microscopy images recorded under the same experimental conditions.

Stability to photobleaching and pulsed excitation at 355 nm

Photobleaching is an undesirable feature of organic based commercial dyes as it prohibits their use in long-term live cell or fixed specimen imaging experiments. Due to the instrumental settings of a modern day confocal microscope, excitation usually occurs in an unspecified tall axial voxel, whilst confocality is achieved via a pinhole in the detection path. This provides the microscopist with an inherent problem when all the observed focal planes are constantly being excited, to some degree, during cell imaging. This results in a rapid decrease in dye intensity due to near continuous excitation and subsequent photobleaching of the cellular stain. To counteract this effect, the intensity window or gain needs to be increased or the applied laser power must be raised gradually. The latter approach results in a greater degree of photobleaching, whilst modulation of the former parameter results in unwanted autofluorescence, rendering intensity based calculations impossible.

In order to assess the photobleaching of such complexes a live-cell imaging experiment was designed to compare the photostability of [**Eu.L^2**] with the commercially available dye, MitoTracker Green, using previously established LSCM experimental settings. Both simultaneous and separate loadings of [**Eu.L^2**] (360 nM, 3h) and MTG (200 nM, 30 min) were examined. Fluorescence intensity was monitored as a function of time for selected emission bands (see ESI).[37] MitoTracker Green was totally photo-bleached (>95%) after only 30 scans (100 seconds), whilst [**Eu.L^2**] retained 70% of its total emission intensity. No significant difference in the rate of photobleaching was observed, when comparing simultaneous or separate dye incubations.

It is well known from consideration of Abbé's law, ($d = \lambda/2(n \sin\theta)$, where $n\sin\theta$ is the numerical aperture (NA) = 1.4 for the immersion system used here, λ is the excitation wavelength and d is the theoretical resolution) that the use of 488 nm vs 355 nm excitation decreases the intrinsic resolution of confocal microscopy from 174 to 126 nm. Indeed, the images obtained in Figure 2 accord with that view. Because of the intrinsic brightness of these Eu probes, the power used in pulsed excitation is only 4 mW (<80 nJ/voxel/acquisition). [38] These experimental conditions are far removed from those used to assess UV damage to tissues and cells, where continuous light exposure persists for several seconds or minutes, and the impact is a steep function of the excitation wavelength, with much less damage occurring above 340 nm.[39] Indeed, in a control experiment examining healthy NIH-3T3 cells loaded with [**Eu.L^2**] (400 nM), following sequential scanning excitation at 355 nm (6 mW) with a 63x objective (NA = 1.4), scanning the same area every 30 minutes for three hours, with a 5-point autofocus determination before each scan (i.e. 23 ms exposure per scan), more than 90% of healthy cells were observed in the field of view. With pulsed excitation at 365 nm (as used in the spectral imaging experiments above), even shorter UV exposure times are achieved.

Conclusions

In summary, we have developed a new series of bright europium dyes and conjugates that serve as luminescent stains for particular organelles within the cell. The complexes exhibit intense, long-lived luminescence, enabling both sensitive detection by microscopy and measurement of their emission profile using time-gated spectral imaging. By permuting the peripheral ligand structure, the complex can be modified allowing stains with different organelle specificities to be found. Thus, the anionic complexes [**Eu.L^1**]$^{3-}$ and [**Eu.L^3**]$^{3+}$ selectively stain the lysosomes, the complex [**Eu.L^2**] bearing ancillary glucamide groups targets the mitochondria, whereas the $GlyArg_7$ peptide conjugate, [**Eu.L^5**]$^{6+}$, mediates delivery to the endoplasmic reticulum. Each europium complex studied, with the exception of [**Eu.L^3**]$^{3+}$, showed no observed cytotoxicity and remained localized in live cells over extended time periods (up to 48h).

The ability to make simple conjugates, *via* substitution of the peripheral aryl substituents allows the creation of a family of tags, exemplified here by the complexes with integral maleimide and biotin moieties. Such systems offer the potential to observe the dynamics of various sub-cellular processes, minimally perturbing cell homeostasis, and do not require the rather lengthy strategies required in labelling with fluorescent recombinant proteins. Indeed, we note that the brightness of these Eu complexes[36] is about the same as the 'red-fluorescent protein', mCherry, which emits at 610 nm (λ_{exc} 587 nm), with an extinction coefficient of 72 $mM^{-1}cm^{-1}$ and a fluorescence quantum yield of 22%. [40]

Taken together, these results herald the introduction of these bright[36] europium complexes as effective stains for cellular imaging, offering improvements in performance to classical fluorescent organic dyes.

Acknowledgement

We thank the ERC for support (DP, SJB, RP; FCC 266804).

Notes and references

[a] *Department of Chemistry, Durham University, South Road, Durham, DH1 3LE, UK . Tel: +44-191-3342033; E-mail: david.parker@dur.ac.uk*
[b] *CISbio Bioassays, Parc Marcel Bioteux, BP84175, Codolet, France*

† Electronic Supplementary Information (ESI) available: synthesis of ligands and complexes and conjugates; microscopy and spectral imaging instrumentation and operating procedures, cell culture, toxicity and excited state quenching experiments . See DOI: 10.1039/b000000x/

1. C. A. Puckett and J. K. Barton, *J. Am. Chem. Soc.*, 2009, **131**, 8738-8739.
2. F. Noor, A. Wüstholz, R. Kinscherf and N. Metzler-Nolte, *Angew.e Chem. Int.l Ed.*, 2005, **44**, 2429-2432.
3. S. Mukhopadhyay, C. M. Barnés, A. Haskel, S. M. Short, K. R. Barnes and S. J. Lippard, *Bioconjugate Chem.*, 2007, **19**, 39-49.
4. O. Aronov, A. T. Horowitz, A. Gabizon, M. A. Fuertes, J. M. Pérez and D. Gibson, *Bioconjugate Chem.*, 2004, **15**, 814-823.
5. F. Noor, R. Kinscherf, G. A. Bonaterra, S. Walczak, S. Wölfl and N. Metzler-Nolte, *ChemBioChem*, 2009, **10**, 493-502.
6. E. J. New, D. Parker, D. G. Smith and J. W. Walton, *Curr. Opin. Chem. Biol*., 2010, **14**, 238-246.
7. E. J. New, A. Congreve and D. Parker, *Chem. Sci.*, 2010, **1**, 111-118.
8. a) B. Wang, Y. Liang, H. Dong, T. Tan, B. Zhan, J. Cheng, K. K-W. Lo, Y. W. Lam, S. H. Cheng, *ChemBioChem*, 2012, **13**, 2729-2737 ; b) E. Baggaley, J. A. Weinstein and J. A. G. Williams, *Coord. Chem. Rev*., 2012, **256**, 1762-1785.
9. C. A. Puckett and J. K. Barton, *J. Am. Chem. Soc.*, 2006, **129**, 46-47.
10. A. R. Cowley, J. Davis, J. R. Dilworth, P. S. Donnelly, R. Dobson, A. Nightingale, J. M. Peach, B. Shore, D. Kerr and L. Seymour, *Chem. Commun.*, 2005, **0**, 845-847.
11. a) R. G. Balasingham, M. P. Coogan and F. L. Thorp-Greenwood, *Dalton Trans*., 2011, **40**, 11663-11674; b) V. Fernandez-Moreira, F. L. Thorp-Greenwood, A. J. Amoroso, J. Cable, J. B. Court, V. Gray, A. J. Hayes, R. L. Jenkins, B. M. Kariuki, D. Lloyd, C. O. Millet, C. F. Williams and M. P. Coogan, *Org. Biomol. Chem*., 2010, **8**, 3888-3901.
12. V. Fernandez-Moreira, F. L. Thorp-Greenwood and M. P. Coogan, *Chem. Commun.*, 2010, **46**, 186-202.
13. S. P.-Y. Li, T. S.-M. Tang, K. S.-M. Yiu and K. K.-W. Lo, *Chem. Eur. J*., 2012, **18**, 13342-13354.
14. a) K. K.-W. Lo, B. T.-N. Chan, H.-W. Liu, K. Y. Zhang, S. P.-Y. Li and T. S.-M. Tang, *Chem. Commun.* 2013, 4271-3; b) K. K. K-W. Lo, A. W-T. Choi and W. H-T. Law, *Dalton Trans.* 2012, **41**, 6021.
15. M.-W. Louie, H.-W. Liu, M. H.-C. Lam, Y.-W. Lam and K. K.-W. Lo, *Chemistry –Eur. J.*, 2011, **17**, 8304-8308.
16. C. A. Strassert, C. H. Chien, M. D. G. Lopez, D. Kourkoulos, D. Hertel, K. Meerholz, L. De Cola, *Angew. Chem. Int. Ed*. 2011, **50**, 946-50.
17. S. Mohandessi, M. Rajendran, D. Magda and L. W. Miller, *Chemistry –Eur. J*., 2012, **18**, 10825-10829.
18. S. V. Eliseeva and J.-C. G. Bunzli, *Chem. Soc. Rev.*, 2010, **39**, 189-227.
19. A. Thibon and V. C. Pierre, *Anal. Bioanal. Chem.*, 2009, **394**, 107-120.
20. D. Parker and J. Yu, *Chem. Commun*. 2005, 3141-3143.
21. J. Yu, D. Parker, R. Pal, R. A. Poole and M. J. Cann, *J. Am. Chem. Soc*., 2006, **128**, 2294-2299.
22. C. P. Montgomery, B. S. Murray, E. J. New, R. Pal and D. Parker, *Acc. Chem. Res.*, 2009, **42**, 925-937.
23. R. Pal, D. Parker and L. C. Costello, *Org. Biomol. Chem.*, 2009, **7**, 1525-1528.
24. J.-C. G. Bünzli, *Chem. Rev.*, 2010, **110**, 2729-2755.
25. C. Song, Z. Ye, G. Wang, J. Yuan and Y. Guan, *Chemistry –Eur. J.*, 2010, **16**, 6464-6472.
26. E. Deiters, B. Song, A.-S. Chauvin, C. D. B. Vandevyver, F. Gumy and J.-C. G. Bünzli, *Chemistry –Eur. J*., 2009, **15**, 885-900.
27. J. W. Walton, A. Bourdolle, S. J. Butler, M. Soulie, M. Delbianco, B. K. McMahon, R. Pal, H. Puschmann, J. M. Zwier, L. Lamarque, O. Maury, C. Andraud and D. Parker, *Chem. Commun.*, 2013, **49**, 1600-1602.
28. J. W. Walton, L. D. Bari, D. Parker, G. Pescitelli, H. Puschmann and D. S. Yufit, *Chem. Commun.*, 2011, **47**, 12289-12291.
29. C. A. Puckett, R. J. Ernst and J. K. Barton, *Dalton Trans.*, 2010, **39**, 1159-1170.
30. T. J. Jess, C. M. Belham, F. J. Thomson, P. H. Scott, R. J. Plevin and G. W. Gould, *Cellular Signalling*, 1996, **8**, 297-304.
31. M. A. West, M. S. Bretscher and C. Watts, *J. Cell Biol*., 1989, **109**, 2731-2739.
32. H. U. Keller, *J. Cellular Physiol.*, 1990, **145**, 465-471.
33. E. J. New and D. Parker, *Org. Biomol. Chem.*, 2009, **7**, 851-855.
34. The quenching efficiency of the donor, [**Eu.**L^6] (3 μM), by the streptavidin-Alexa-Fluor633 acceptor was assessed *in vitro* (0.1 M NaCl, pH 7.4) by monitoring the change of the Eu emission lifetime as a function of added acceptor concentration, over the range 30 nM to 1.6 μM. The second order rate constant, k_2 , defining this energy transfer quenching process was 0.62 $mM^{-1}s^{-1}$, with τ_o = 1.02 ms. These values are very similar to those observed for the parent europium phosphinate complex with a very similar cyanine dye acceptor [27].
35. H. E. Rajapakse, N. Gahlaut, S. Mohandessi, D. Yu, J. R. Turner and L. W. Miller, *Proc. Natl. Acad. Sci. USA*, 2010, **107**, 13582.
36. A practical expression reflecting the observed brightness, *B*′, of a luminescent complex in a time gated spectroscopy or microscopy experiment using pulsed excitation at a given wavelength, λ, is:

$$B'(\lambda,c) = \eta\varepsilon\phi\int e^{-kt}.dt$$

where c is the complex loading concnetration, λ is the applied excitation wavelength, η is the cellular accumulation constant. The integral has limits (t_{acq} + t_d) and t_d, in which k is the radiative rate constant, t_{acq} is the spectrocopic integration time or microscopy acquisition time and t_d is the delay time following pulsed excitation.
37. Thus, (x*y*t) experiments were undertaken in a continuous mode using a 1-frame, 4-line averaged scan (total time 3.5s/scan) at 700 Hz, operating in a bidirectional mode with a 1024x1024 frame size, a pixel size of 132x132 nm and depth of 0.78 μm, using 488 and 355 nm lasers, each operating at 4 mW.
38. In the Figures shown here, four consecutive scans (400 MHz) were taken over 3.5 seconds, examining a 1024x1024 area (pixel size 132 x 132nm x 0.78μm depth) with a 63x objective giving a S/N of 40:1, exposing each pixel to light for only 10 microseconds.
39. J. C. F. Wong and A. Parisi, 'Assessment of ultraviolet radiation exposures in photobiological experiments', in: Protection Against the Hazards of UVR Internet Conference, 18 Jan - 5 Feb 1999 ttp://eprints.usq.edu.au/1279/.
40. N. C. Shaner, R. E. Campbell, P. A. Steinbach, B. N. G. Giepmans, A. E. Palmer and R. Y. Tsien, *Nature Biotechnology* 2004, **22**, 1567.